

Superheavy Element Flerovium (Element 114) Is a Volatile Metal

Alexander Yakushev,^{†,‡} Jacklyn M. Gates,^{†,‡,⊙} Andreas Türler,^{†,▲} Matthias Schädel,^{‡,▼} Christoph E. Düllmann,^{*,‡,§,||} Dieter Ackermann,[‡] Lise-Lotte Andersson,[⊥] Michael Block,[‡] Willy Bröchle,[‡] Jan Dvorak,^{#,∇,★} Klaus Eberhardt,[§] Hans G. Essel,[‡] Julia Even,[§] Ulrika Forsberg,[⊙] Alexander Gorshkov,^{†,■} Reimar Graeger,^{†,⊗} Kenneth E. Gregorich,[#] Willi Hartmann,[‡] Rolf-Dietmar Herzberg,[⊥] Fritz P. Heßberger,^{‡,||} Daniel Hild,[§] Annett Hübner,[‡] Egon Jäger,[‡] Jadambaa Khuyagbaatar,^{‡,||} Birgit Kindler,[‡] Jens V. Kratz,[§] Jörg Krier,[‡] Nikolaus Kurz,[‡] Bettina Lommel,[‡] Lorenz J. Niewisch,[§] Heino Nitsche,^{#,∇} Jon Petter Omtvedt,[◆] Edward Parr,[⊥] Zhi Qin,[¶] Dirk Rudolph,[⊙] Jörg Runke,[‡] Brigitta Schausten,[‡] Erwin Schimpf,[‡] Andrey Semchenkov,[◆] Jutta Steiner,[‡] Petra Thörle-Pospiech,^{§,||} Juha Uusitalo,[◇] Maciej Wegrzecki,[●] and Norbert Wiehl^{§,||}

[†]Institut für Radiochemie, TU Munich, 85748 Garching, Germany

[‡]GSI Helmholtzzentrum für Schwerionenforschung, 64291 Darmstadt, Germany

[§]Institut für Kernchemie, Johannes Gutenberg University Mainz, 55099 Mainz, Germany

^{||}Sektion SHE Chemie, Helmholtz Institute Mainz, 55099 Mainz, Germany

[⊥]Department of Physics, University of Liverpool, L69 7ZE Liverpool, U.K.

[#]Nuclear Science Division, Lawrence Berkeley National Laboratory, Berkeley, California 94720-8169, United States

[∇]Chemistry Faculty, University of California, Berkeley, California 94720-1460, United States

[⊙]Department of Physics, Lund University, 221 00 Lund, Sweden

[◆]Department of Chemistry, University of Oslo, 0315 Oslo, Norway

[¶]Institute of Modern Physics, 730000 Lanzhou, People's Republic of China

[◇]Department of Physics, University of Jyväskylä, 40014 Jyväskylä, Finland

[●]Institute of Electron Technology, 02-668 Warsaw, Poland

ABSTRACT: The electron shell structure of superheavy elements, i.e., elements with atomic number $Z \geq 104$, is influenced by strong relativistic effects caused by the high Z . Early atomic calculations on element 112 (copernicium, Cn) and element 114 (flerovium, Fl) having closed and quasi-closed electron shell configurations of $6d^{10}7s^2$ and $6d^{10}7s^27p_{1/2}^2$, respectively, predicted them to be noble-gas-like due to very strong relativistic effects on the $7s$ and $7p_{1/2}$ valence orbitals. Recent fully relativistic calculations studying Cn and Fl in different environments suggest them to be less reactive compared to their lighter homologues in the groups, but still exhibiting a metallic character. Experimental gas–solid chromatography studies on Cn have, indeed, revealed a metal–metal bond formation with Au. In contrast to this, for Fl, the formation of a weak bond upon physisorption on a Au surface was inferred from first experiments. Here, we report on a gas–solid chromatography study of the adsorption of Fl on a Au surface. Fl was produced in the nuclear fusion reaction $^{244}\text{Pu}(^{48}\text{Ca}, 3-4n)^{288,289}\text{Fl}$ and was isolated in-flight from the primary ^{48}Ca beam in a physical recoil separator. The adsorption behavior of Fl, its nuclear α -decay product Cn, their lighter homologues in groups 14 and 12, i.e., Pb and Hg, and the noble gas Rn were studied simultaneously by isothermal gas chromatography and thermochromatography. Two Fl atoms were detected. They adsorbed on a Au surface at room temperature in the first, isothermal part, but not as readily as Pb and Hg. The observed adsorption behavior of Fl points to a higher inertness compared to its nearest homologue in the group, Pb. However, the measured lower limit for the adsorption enthalpy of Fl on a Au surface points to the formation of a metal–metal bond of Fl with Au. Fl is the least reactive element in the group, but still a metal.

1. INTRODUCTION

Superheavy elements (SHEs) are unique in two respects. Their nuclei exist only due to nuclear shell effects, and their electron structure is influenced by increasingly important relativistic effects.^{1–3} Syntheses of SHE with a proton number Z up to 118

have been reported.⁴ Elements with $Z = 104–112$ are members of the 6d series in the periodic table of the elements. The 7p

Received: October 24, 2013

Published: January 23, 2014

valence shell is expected to be filled in the elements with $Z = 113$ – 118 . The discovery of elements with $Z = 114$ and $Z = 116$ was recently officially accepted, and they were named flerovium (Fl) and livermorium (Lv), respectively.⁵ Lighter transactinides with $Z = 104$ – 108 were experimentally shown to be members of groups 4 through 8 of the periodic table of the elements.⁶ Because of the increasing nuclear charge in SHEs, the velocity of electrons in the inner shells approaches the speed of light. This causes a relativistic increase in the electron mass. Hence, the spherical s and $p_{1/2}$ electron shells, having a nonzero electron density at the nucleus, contract in space and become stabilized in energy. This is the so-called direct relativistic effect. As a consequence, the nonspherical atomic orbitals (AOs) $p_{3/2}$, d , f , etc. are more efficiently screened from the nucleus, thus undergoing destabilization in energy and expansion in space: the indirect relativistic effect. Finally, the third effect is a spin-orbit splitting of AOs with $l > 0$. All three relativistic effects scale approximately with Z^2 for valence electron shells and are thus most pronounced in SHEs.

Beyond the classical closed-shell configuration $6d^{10}7s^2$ in copernicium (Cn, element 112), the very large spin-orbit splitting in $7p$ AOs and the strong relativistic stabilization of the $7p_{1/2}$ AOs result in a quasi-closed-shell configuration $7s^27p_{1/2}^2$ in Fl. This, together with the relativistic stabilization of the $7s$ AOs renders both Cn and Fl to be more inert than their lighter homologues. According to early atomic calculations by Pitzer,⁷ the promotion energy to the valence state electron configuration $s^2 \rightarrow sp$ in Cn and $p_{1/2}^2 \rightarrow p^2$ in Fl will not be compensated by the energy gain of the chemical bond formation. He concluded that both Cn and Fl are very inert, like noble gases or volatile liquids bound by dispersion forces only. At the same time, other approaches, e.g., extrapolations along groups 12 and 14, indicate a noble, but metallic, character for these elements, more similar to their homologues mercury and lead, respectively.⁸

The discovery of neutron-rich isotopes of Cn and Fl with half-lives, $T_{1/2}$, in the range of seconds⁹ aroused new interest for theoretical predictions of the adsorption behavior for Cn and Fl on various surfaces and called for first experimental efforts. Eichler quantified the adsorption interaction of the hypothetically noble metals Cn and Fl with transition-metal surfaces¹⁰ based on an empirical model developed by Miedema and Nieuwenhuys.¹¹ Adsorption enthalpies of Fl on different transition-metal surfaces were predicted to be higher by approximately $100 \text{ kJ}\cdot\text{mol}^{-1}$ than those of Cn on these surfaces.¹⁰ Experimental studies on the adsorption of Rn on various transition-metal surfaces were undertaken, serving as a model for a hypothetical *noble-gas-like* behavior of elements Cn and Fl.¹² The authors of ref 12 applied an extended Miedema model for estimating the strength of Cn and Fl adsorption on those metals. The adsorption of Fl on a metal surface was predicted to be stronger than that of Cn. However, if Cn and Fl would exhibit *noble-gas-like* properties, their adsorption enthalpy values would be much lower than in the case of a *noble-metal-like* behavior.¹² More recent molecular, cluster, and solid-state relativistic calculations on these elements suggest Cn and Fl to be more inert than their lighter homologues in the groups, but still reveal a metallic character,^{13–15} e.g., in MM' interactions ($M = \text{Cn}$ or Fl ; $M' = \text{metal}$, e.g., Au). In contrast to Pitzer's conclusion, Fl is now expected to provide both $7p_{1/2}$ and $7p_{3/2}$ AOs for metal–metal interactions. By considering the hypothetical solid state of Fl, the authors of ref 16 found that Fl is the most inert element in group 14, but reveals a metallic

character, with the cohesive energy being 0.5 eV/atom . Therefore, a purely van der Waals type interaction upon adsorption on metal surfaces, as is typical for noble gases, is no longer anticipated for either element. Hence, the determination of the adsorption enthalpy of the interaction of Cn and Fl with metal surfaces is a suitable experimental method to discriminate between a *noble-gas-like* and a *noble-metal-like* behavior. The adequate experimental approach is detection of atoms (molecules) adsorbed inside a gas chromatography channel within a broad temperature range. The chromatography channel is made of silicon detectors for the detection of α particles and spontaneous fission (SF) fragments. This approach was successfully applied for the first time in chemical studies on HsO_4 .¹⁷ Cn was investigated by thermochromatography on a Au surface. Five α -SF decay chains starting with ^{285}Cn were found by irradiating a ^{242}Pu target with a ^{48}Ca ion beam.^{18,19} The evaluated adsorption enthalpy of Cn on a Au surface ($-\Delta H_{\text{ads}}^{\text{Au}}(\text{Cn}) = 52_{-3}^{+4} \text{ kJ}\cdot\text{mol}^{-1}$, at the 68% confidence level (68% c.l.)) points at the formation of a weak metal–metal bond with Au.¹⁹ The determined adsorption enthalpy value for Cn is significantly lower than that for the nearest homologue in the group Hg ($-\Delta H_{\text{ads}}^{\text{Au}}(\text{Hg}) = 98 \pm 3 \text{ kJ}\cdot\text{mol}^{-1}$, ref 20), however, in agreement with the limit ($-\Delta H_{\text{ads}}^{\text{Au}}(\text{Cn}) < 60 \text{ kJ}\cdot\text{mol}^{-1}$), which was found in previous experiments.²¹ Thus, Cn exhibits *noble-metal-like* properties,^{18,19} in line with trends established by the lighter homologues in group 12, and in good agreement with recent theoretical calculations.^{14,15}

In recent years, Fl isotopes with half-lives of the order of seconds have been discovered.^{9,22–26} The most long-lived currently known Fl isotopes, produced in the nuclear fusion reaction $^{48}\text{Ca} + ^{244}\text{Pu}$ are ^{289}Fl ($T_{1/2} = 2.1 \text{ s}$) and ^{288}Fl ($T_{1/2} = 0.69 \text{ s}$), which are formed upon the evaporation of three or four neutrons from the excited compound nucleus, respectively. These half-lives are long enough for current gas-phase chromatography experiments with single atoms of superheavy elements.⁶ Besides the short half-lives, minute production rates^{4,22} also complicate chemical studies of superheavy elements. Beyond Cn, only a single chemical experimental study, focused on Fl, is reported to date.²⁷ Three atoms from two Fl isotopes, $^{287,288}\text{Fl}$, were found to pass Au surfaces kept at room temperature and progressively getting colder, until they decayed at temperatures of -88 , -90 , and $-4 \text{ }^\circ\text{C}$. A Monte Carlo simulation of the observed behavior resulted in $-\Delta H_{\text{ads}}^{\text{Au}}(\text{Fl}) = 34_{-11}^{+54} \text{ kJ}\cdot\text{mol}^{-1}$ at the 95% confidence level (95% c.l.). The rather low most probable value of $-\Delta H_{\text{ads}}$ was interpreted by the authors as evidence for the formation of a weak physisorption bond between atomic Fl and a Au surface.²⁷ However, the large uncertainty of the reported $-\Delta H_{\text{ads}}$ covers almost the entire range from a typical *metallic* (cf. $-\Delta H_{\text{ads}}^{\text{Au}}(\text{Hg}) = 98 \pm 3 \text{ kJ}\cdot\text{mol}^{-1}$, ref 20) to a *noble-gas-like* behavior (cf. $-\Delta H_{\text{ads}}^{\text{ice}}(\text{Rn}) = 19.2 \pm 1.6 \text{ kJ}\cdot\text{mol}^{-1}$, ref 28) and hence, the result does not allow for a clear discrimination between a *metallic*- and *noble-gas-like* behavior. The longer-lived isotope ^{289}Fl could not be identified due to a high background from Rn isotopes and their decay products, disturbing an unambiguous identification of decay chains starting with ^{289}Fl .²⁷ Both, nuclear as well as chemical, aspects of the experiment reported in ref 27 have been criticized; see ref 29. The predicted similarity of a hypothetical *noble-gas-like* behavior of Fl to that of Rn calls for applying physical pre-separation methods to separate Cn and Fl from Rn. Its decay products caused the main background in the α spectra in ref 27. A first attempt using physical pre-separation was performed at the

Dubna Gas-Filled Recoil Separator (DGFRS), but failed to observe Fl.³⁰ The question of whether Fl resembles more closely a noble gas or a noble metal is among the most pressing ones in concurrent superheavy element chemistry and needs to be solved experimentally in a more sensitive and detailed study.

Here, we report on chemical studies of Fl after pre-separation with TASCA, which led to the observation of two Fl atoms.

2. EXPERIMENTAL SECTION

To isolate Fl, we exploited a combination of the TransActinide Separator and Chemistry Apparatus^{25,31,32} (TASCA) and the Cryo-Online Multidetector for Physics And Chemistry of Transactinides (COMPACT).³³ TASCA served for suppression of the primary beam and of the background from Rn isotopes and their decay products. This allowed the observation of the characteristic radioactive decay of Fl and its (grand)-daughters under significantly improved background reduction compared to previous studies²⁷ performed without pre-separation.

The gas chromatography and detection system comprised two COMPACT detector arrays that were placed behind TASCA. The experimental setup is schematically shown in Figure 1.

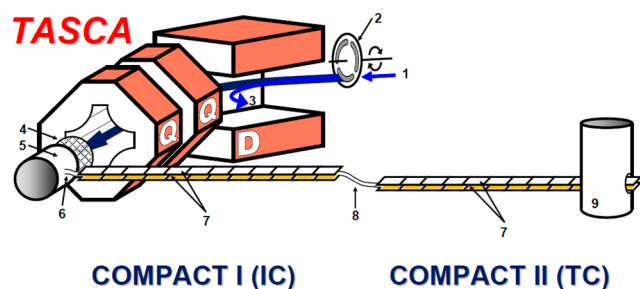


Figure 1. Schematic drawing of the TASCA-COMPACT² arrangement used for the gas chromatographic investigation of the volatility of Fl and its reactivity toward a Au surface. The ⁴⁸Ca beam (1) passed through the rotating ²⁴⁴Pu target (2) assembly. The separator TASCA consists of one dipole (D), where unwanted nuclear reaction products (3) were deflected, and two quadrupole (Q) magnets. At the exit of TASCA, a vacuum window (4) separated the low pressure required in TASCA from the high pressure applied in the recoil transfer chamber (RTC) (5). After passing the vacuum window, Fl was thermalized in the gas inside the RTC and was transported in its elemental state with the carrier gas through a 2 cm long PTFE tube (6) into a series of two COMPACT detector arrays (7) connected by a 30 cm long polytetrafluoroethylene (PTFE) capillary (8) (2 mm i.d.). A negative temperature gradient was applied along COMPACT II using a liquid nitrogen cryostat (9) at the exit.

A ⁴⁸Ca¹⁰⁺ beam of typically 2·10¹² particles·s⁻¹ was accelerated by the UNiversal Linear ACcelerator (UNILAC) at the GSI, Darmstadt, Germany, to an energy of 259.4 MeV. In total, a projectile dose of 4 × 10¹⁸ particles was collected. The projectiles first passed through (2.50 ± 0.05) μm thick Ti target-backing foils, and then entered the ²⁴⁴PuO₂ targets prepared by molecular plating and mounted on a rotating wheel.^{34,35} The target wheel consisted of three segments (1.7 cm² area each) covered with 440, 771, and 530 μg cm⁻² ²⁴⁴Pu, respectively. The isotopic composition was 97.9% ²⁴⁴Pu; 1.3% ²⁴²Pu; 0.7% ²⁴⁰Pu; <0.1% other. The target wheel rotated with 2000 rev min⁻¹ and was synchronized with the beam macrostructure to distribute each 5 ms long beam pulse evenly over one target segment.³⁶ In complete nuclear fusion reactions, ²⁹²Fl* compound nuclei at an excitation energy, E*, of 40–45 MeV were formed.^{37,38} After deexcitation by evaporation of three or four neutrons, the resulting ^{288,289}Fl nuclei recoiled from the target into the separator TASCA operated in the “Small Image Mode”.³² The primary beam and unwanted nuclear reaction products were deflected inside the dipole magnet to a beam stop, while Fl was guided to the focal plane (Figure 1). Magnets were

set to focus ions with a magnetic rigidity, B·ρ, of 2.27 T·m into a (~3 × 5) cm² area in TASCA’s focal plane. Monte Carlo simulations indicate that 35% of the Fl ions reached this area.^{25,39} There, they penetrated a (40 × 30) mm² large MYLAR window of (3.3 ± 0.1) μm in thickness mounted on a 1 mm thick supporting grid of 80% geometrical transparency and entered the Recoil Transfer Chamber (RTC).^{31,40} The window separated the low-pressure region in TASCA (0.5 mbar) from the high-pressure one in the RTC (~900 mbar). In the 29 cm³ large RTC, made from polytetrafluoroethylene (PTFE), the Fl ions were thermalized in a dried (measured dew point below -60 °C) gas mixture (He/Ar = 70:30; gas purities: 99.9999% (He) and 99.999% (Ar)), which flushed the RTC at a total flow rate of 1300–1800 mL·min⁻¹. The Ar admixture (30%) in the carrier gas served to increase the stopping power inside the RTC, which allowed minimizing the RTC volume. Short-lived Hg and Pb isotopes, chemical homologues of Cn and Fl, were produced using ¹⁴²Nd and ¹⁴⁴Sm targets, respectively. By producing pulses of ¹⁸²Hg recoils (0.4 s beam on and 50 s beam off) and measuring the time delay until their decay in COMPACT, the most probable transport time to COMPACT I was determined to be (0.81 ± 0.06) s at a gas flow rate of 1300 mL·min⁻¹.

Volatile species, including Fl, which was transported in its elemental state, were flushed with this carrier gas mixture through a 2 cm long PTFE tube (3 mm inner diameter, i.d.) into the first of the two COMPACT detector arrays (Figure 1). Each array consisted of 32 pairs (gap: 0.6 mm) of (1 × 1) cm² large positive-intrinsic-negative (PIN) epitaxial silicon photodiodes with an active area of (9.7 × 9.8) mm² and an effective thickness of 150 μm. The calculated geometrical efficiencies for detecting an α particle or spontaneous fission from atoms present inside a detector array were 93% and ~100%, respectively. All detectors were covered by a (35–50) nm thick Au layer deposited by evaporation. COMPACT I was operated as an isothermal chromatography (IC) detector array at room temperature (21 °C). It retained metallic elements that form a strong chemical bond with Au at room temperature, such as Pb or Hg. Chemical species that did not adsorb in COMPACT I exited, passed through a 30 cm long PTFE capillary (2 mm i.d.), and entered COMPACT II. COMPACT II was added 5 days after the start of the 29-day long experiment. A negative temperature gradient from +20 to -162 °C was applied along COMPACT II (thermochromatography detector array, TC) using a liquid nitrogen cryostat at the exit. For the first 3 days of operation, the lowest temperature in COMPACT II was -86 °C due to a weak thermal contact between the detector array and the cryostat. Volatile and inert elements pass COMPACT I and adsorb in COMPACT II at characteristic low temperatures. The energy resolution of the COMPACT detectors was ≈120 keV (fwhm). A higher resolution could not be reached because α particles are emitted isotropically at various angles in the narrow channel. Depending on their incident angle, they pass through different effective thicknesses of detector dead layer and gas, thus undergoing energy loss to a different degree, before entering the active detector area. Accordingly, α peaks show characteristic low-energy tailing. All transported species came in contact inside and downstream of the RTC exclusively with PTFE and Au surfaces. This setup allowed for detecting species in a wide range of volatilities, namely, from the low-volatile Pb to the noble gas Rn. If Fl behaves like a metal, it will adsorb in COMPACT I; if, in contrast, Fl rather behaves like a noble gas, it will deposit at a much lower temperature in COMPACT II. The overall transfer yield from TASCA to COMPACT was measured with short-lived Hg and Pb isotopes. To this end, the rate at which Hg atoms entered the RTC was determined by implanting them into a (58 × 58) mm² double-sided silicon strip detector. A subsequent experiment, in which the atoms were thermalized in the RTC and transported to COMPACT at a flow rate of 1300 mL·min⁻¹, yielded that the decay of 27% of all Hg atoms entering the RTC was observed in COMPACT. For Pb isotopes, this value was lower (20%), due to additional adsorption losses of the less volatile Pb on the walls of the RTC and the connecting tube. The distributions of ¹⁸²Hg and ¹⁸⁵Pb isotopes in COMPACT were measured before and after the Fl measurement and found to be reproducible. Between these measurements, neither of the two

COMPACT arrays mounted in the gas loop was opened. COMPACT II was warmed up every 2–3 days to remove the thin ice layer that formed on detectors held at temperatures below -75 °C.

3. RESULTS

A search for correlated decay chains starting from $^{288,289}\text{Fl}$ was performed. The search conditions were the following: in the case of ^{288}Fl , we searched for a 9.6–10.1 MeV α particle, followed within 1 s by a >20 MeV fission fragment, which was registered in either the same or an adjacent detector pair, where the first α particle was found. For ^{289}Fl , we searched for a 9.6–10.1 MeV α particle, followed by a 8.8–9.3 MeV α particle, followed by a >20 MeV fission fragment, all within 200 s. The search was extended to all detector pairs downstream of the one where the mother decay was observed, because the daughter of Fl, Cn, is known to be a volatile metal and thus can be transported by gas flow along the detector channel. This procedure revealed two correlated decay chains, which we show in Figure 2.

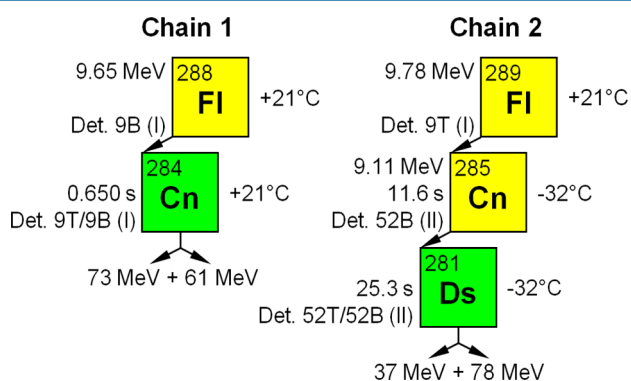


Figure 2. Observed correlated decay chains assigned to Fl. Left-hand side of the boxes: α -particle energy, lifetime of the nucleus, and detector number in which the signal was measured (“T” and “B” are top and bottom detectors of a detector pair, respectively). (I) and (II) denote COMPACT I and COMPACT II, respectively. Energies of SF fragments are given below the boxes. No pulse-height defect correction was applied to the SF energies. Right-hand side of the boxes: temperature of the detector that registered the event.

Both members of chain #1 were observed in detector pair #9 in COMPACT I, which was kept at 21 °C. The members of chain #2 were found distributed over both COMPACT arrays: the α particle of the mother nucleus initiating the chain was detected in detector #9 “top” in COMPACT I. The last two members of the chain were detected in detector pair #52 in COMPACT II at -32 °C. On the basis of the good agreement of the nuclear properties of our observed chains with decay properties reported from $^{288,289}\text{Fl}$ synthesis experiments^{4,23,25}, we assign chain #1 to the decay of $^{288}\text{Fl} \rightarrow ^{284}\text{Cn}$ and chain #2 to $^{289}\text{Fl} \rightarrow ^{285}\text{Cn} \rightarrow ^{281}\text{Ds}$, produced in the 4n and 3n evaporation channel, respectively. A search for SF decays ($E > 20$ MeV) revealed two additional events. In total, only these four SF events were registered—all with two coincident fission fragments. No “single” fission fragment with $E_{\text{frag}} > 20$ MeV was detected. The SF events, for which no α -decay precursor was found, appeared at temperatures of +21 °C (COMPACT I, det. 1T/1B, 83/83 MeV) and -86 °C (COMPACT II, det. 64T/64B, 24/85 MeV). A definite assignment of these two SF events to a certain element is not possible as SF is an unspecific decay mode.

The observed α energies in the decay chains are somewhat lower compared to the energies registered in earlier experiments in a focal plane detector, into which the $^{288,289}\text{Fl}$ were implanted.^{22,23,25} This is due to energy loss in the gas layer, which the α particles penetrate in roughly half of all cases, and is in agreement with a long tail of α peaks toward the low-energy side (Figure 3). Such an effect was observed in all our

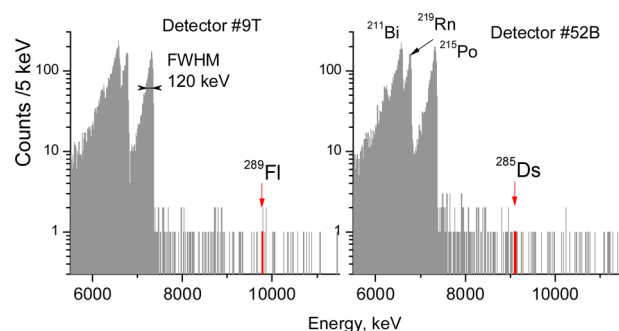


Figure 3. Spectra measured in detector #9T of COMPACT I (left panel) and detector #52B of COMPACT II (right panel) during 22 days. α decays from ^{289}Fl and ^{285}Ds are shown in red.

previous chemistry experiments, where similar cryodetectors were used, see refs 17 and 33. The asymmetric broadening of α peaks toward low energy can be understood as being due to the energy loss of particles penetrating the gas channel at shallow angles.

Because of the extremely low background from α particles and especially from SF fragments, the observed decay chains are highly significant. The probabilities for a random origin, unrelated to the decay of Fl, are only 6.3×10^{-6} (chain #1) and 1.3×10^{-6} (chain #2). Figure 3 shows the total α spectra measured during 22 days in detector #9T (COMPACT I) (left panel) and in detector 52B (COMPACT II) (right panel), where members of the second decay chain were registered. The entries of two α particles belonging to ^{289}Fl and ^{285}Cn , the members of chain #2, are marked, distributed over two COMPACT detectors. The only peaks visible in these spectra arise from the decay chain $^{219}\text{Rn} \rightarrow ^{215}\text{Po} \rightarrow ^{211}\text{Bi}$. Small amounts of ^{219}Rn were added to the carrier gas to allow for an online monitoring of the detection system and to provide α calibration data. No peaks are present in the spectra above the highest energy originating from the ^{219}Rn chain, i.e., above 7.5 MeV. This illustrates nicely the power of physical preseparation by a recoil separator in a chemistry experiment.

4. DISCUSSION

In Figure 4, we show the temperature profile in the main part of the experiment (panel a) together with the measured distribution (solid bars) of Pb (panel b), Hg (panel c), and Rn (panel d). Also shown are the positions at which the members of the two Fl decay chains were observed (e). Monte Carlo Simulations⁴¹ (MCS) of the migration of Pb, Hg, Rn, Cn, and Fl along the chromatography detectors were performed with 10 000 atoms for each element. The distribution pattern of Rn in COMPACT II was simulated using the literature value ($-\Delta H_{\text{ads}}^{\text{ice}}(\text{Rn}) = 20 \text{ kJ}\cdot\text{mol}^{-1}$, ref 28). Pb and Hg interact strongly with a Au surface ($-\Delta H_{\text{ads}}^{\text{Au}}(\text{Pb}) > 295 \text{ kJ}\cdot\text{mol}^{-1}$ (ref 42), and $-\Delta H_{\text{ads}}^{\text{Au}}(\text{Hg}) = (98 \pm 3) \text{ kJ}\cdot\text{mol}^{-1}$ (ref 20)), and their deposition temperatures on a Au surface are well above room temperature. The similarity in the observed distribution

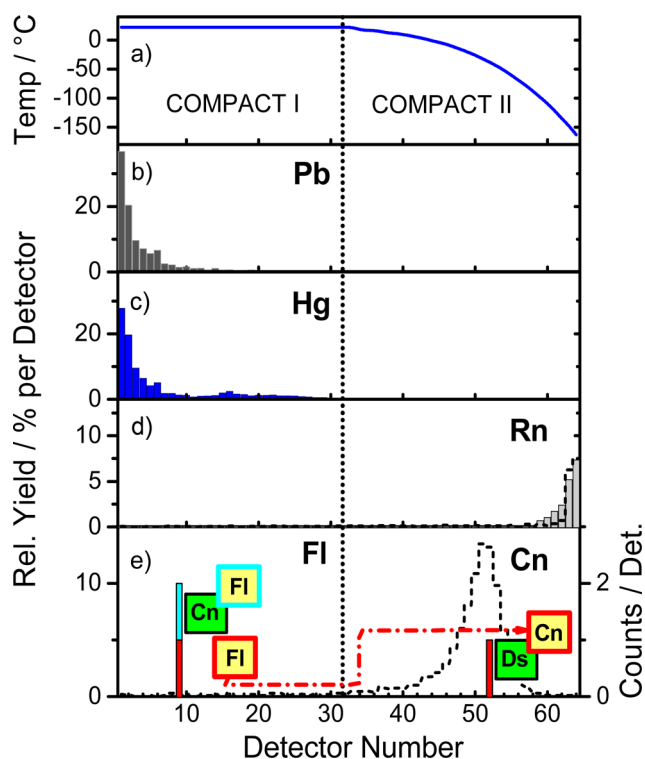


Figure 4. Observed gas chromatography behavior of FI and Cn in COMPACT compared to that of Pb, Hg, and Rn. Measured distributions (bars) of ^{185}Pb (panel b), ^{182}Hg (panel c), and ^{219}Rn (panel d) together with the temperature profile in the main part of the experiment (panel a) are shown. The positions where the α particles from the members of the decay chains were observed are shown in (e): chain #1 – event in light blue in the histogram, corresponding to the light-blue bordered inserted box; chain #2 – events in red/red-bordered boxes. The fissions terminating the chains were observed in the same detector pairs as precursor α particles from FI in chain #1 or from Cn in chain #2. The dashed lines show the results of Monte Carlo simulations for Rn and Cn using literature values (refs 28 and 19) for $-\Delta H_{\text{ads}}$.

patterns for Hg and Pb, which have significantly different adsorption enthalpies on a Au surface, points at the diffusion-controlled nature of the adsorption process. The diffusion to the wall controls the process for both Pb and Hg, and they adsorb upon first contact with the surface at the beginning of COMPACT I. Using MCS, a lower limit of $-\Delta H_{\text{ads}}^{\text{Au}} > 64 \text{ kJ}\cdot\text{mol}^{-1}$ was deduced for both Pb and Hg.

In the following part, we discuss the adsorption scenarios for the two FI atoms. Both α decays from FI have been found in the IC section, where short-lived isotopes of the metallic elements Pb and Hg were deposited. For the unknown adsorption behavior of FI, three possible cases can be discussed. (i) FI is not very volatile and reacts strongly with Au. Then, the distribution pattern in COMPACT should be similar to that of its nearest lighter homologue Pb. However, both decays of FI were found in the detector pair #9, while more than 90% of Pb was deposited on the first eight detector pairs. This fact points to a weaker reactivity of FI with Au compared to Pb. (ii) FI does not exhibit a metallic character but interacts with Au by weak dispersion forces. In that case, most of the FI should pass COMPACT I and decay at low temperatures in COMPACT II. Decays inside COMPACT I, occurring predominantly due to decay-in-flight, will be distributed evenly along the whole detector array. Rn is a typical representative for such a behavior.

It is not deposited until very low temperatures are reached. In fact, most of the Rn was flushed out after passing both COMPACT arrays. In this case, FI decays would be predominantly detected in COMPACT II. (iii) FI may behave as a volatile metal and decays upon the adsorption on a Au surface in one of the two COMPACT arrays, with the deposition temperature and hence position depending on its adsorption enthalpy value, similar to a behavior observed for Cn.

In chain #1 originating from ^{288}Fl , the SF decay from ^{284}Cn was registered, after a lifetime of 650 ms, in the same detector pair as the α decay of the mother nuclide ^{288}Fl . A ^{284}Cn atom interacting with a Au surface with $-\Delta H_{\text{ads}}^{\text{Au}}(\text{Cn}) = 52 \text{ kJ}\cdot\text{mol}^{-1}$ needs about 135 ms to be transported 1 cm downstream in COMPACT I by the carrier gas. Within 650 ms, a ^{284}Cn atom, either residing adsorbed on the surface or being immersed in the gas, would be transported a few centimeters downstream in the detector channel. The fact that ^{284}Cn remained at the same position during its entire lifetime is indicative of its implantation into the detector as a recoiling atom in the α decay of ^{288}Fl . This is expected in about 50% of all α decays. It is due to the nuclear recoil from the nuclear decay of the mother atom with the α particle being emitted away from the surface of the detector on which the mother atom is adsorbed. As the recoil range of α -decay products is very small, this implies that indeed the mother atom, ^{288}Fl , was adsorbed on the detector surface when it decayed, and that the position where the decay was observed is indicative of a chemical interaction of FI with the Au surface. In chain #2 originating from ^{289}Fl , the last two members, starting from the daughter nucleus ^{285}Cn , were found in detector pair #52 at a temperature of $\sim -32^\circ\text{C}$. Apparently, upon α decay of the mother nucleus, the daughter ^{285}Cn recoiled into the gas stream. During its lifetime of 11.6 s, it was transported along the detector channel into COMPACT II. As shown in Figure 4e, the observed adsorption position for ^{285}Cn agrees well with the calculated deposition pattern for this Cn isotope using the experimentally measured adsorption enthalpy.¹⁹ This corroborates our assignment of the last two members to $^{285}\text{Cn} \rightarrow ^{281}\text{Ds}$ and hence that of the mother being ^{289}Fl .

Both observed FI decays were registered in the isothermal section, in COMPACT I, while zero decays were observed in COMPACT II. Considering the low experimental statistics, a method of calculating confidence intervals for experiments with small event numbers was applied.⁴³ The numbers of events, which were detected in COMPACT I and COMPACT II, are $D = 2$ and $N = 0$, where we use the notation as in ref 43. For the evaluation of confidence levels using Poisson statistics, D and N can vary from 0 to 2, with $D + N = 2$. Lower (R_{lo}) and upper (R_{hi}) limits for the ratio $R = N/D$ can be calculated for different confidence intervals, as well as the most probable value of R , R_{max} (ref 43). Thus, the upper limit R_{hi} corresponds to the maximum value of N , N_{hi} , within the selected confidence interval and, therefore, to the minimum value of D , D_{lo} . Similarly, the lower limit R_{lo} corresponds to the minimum value of N , N_{lo} , and to the maximum value of D , D_{hi} , within the selected confidence interval. From the experiment, we obtained the most probable value of R as $R_{\text{max}} = 0$, resulting in limits $R_{\text{lo}} = 0$ and $R_{\text{hi}} = 1.650$ for the 95% confidence level (95% c.l.). These values correspond to $N_{\text{hi}} = 1.24$ and $D_{\text{lo}} = 0.76$. Thus, the experimental values D and N are Poisson distributed within the intervals: $0.76 < D < 2$ and $0 < N < 1.24$ at the 95% confidence level. The minimum value for the number of events D , which

are detected in COMPACT I at this limit, is 0.76 out of 2, i.e., 38%. To convert this into a limit for $-\Delta H_{\text{ads}}^{\text{Au}}(\text{Fl})$, the deposition pattern for both observed Fl isotopes along the entire COMPACT array was simulated for various values of $-\Delta H_{\text{ads}}^{\text{Au}}(\text{Fl})$ using MCS.⁴¹ All simulations with $-\Delta H_{\text{ads}}^{\text{Au}}(\text{Fl}) \geq 48 \text{ kJ}\cdot\text{mol}^{-1}$ resulted in distributions where at least 38% of all events decayed in COMPACT I. Therefore, $-\Delta H_{\text{ads}}^{\text{Au}}(\text{Fl}) > 48 \text{ kJ}\cdot\text{mol}^{-1}$ was found as a lower limit for the adsorption enthalpy of Fl on a Au surface at 95% c.l. Similar calculations were performed for 90% and 68% confidence intervals, resulting in limits of 49 and 50 kJ/mol, respectively.

5. CONCLUSION

A gas-phase chromatography experiment with Fl was performed. Two atoms were registered. The observed behavior of Fl in the chromatography column indicates that Fl is less reactive than Pb. The estimated minimum value of $-\Delta H_{\text{ads}}^{\text{Au}}(\text{Fl}) > 48 \text{ kJ}\cdot\text{mol}^{-1}$ reveals a *metallic* character upon adsorption on a Au surface due to the formation of a metal–metal bond, which is at least as strong as that of Cn.^{18,19} The observed behavior is in agreement with results of recent fully relativistic calculations on the adsorption of Fl on a Au surface,^{13–15} but disagrees with an observation of adsorption of Fl on a Au surface merely due to physisorption.²⁷ To conclude, the present experimental study has established that Fl is a *volatile metal*, the least reactive one in group 14. It is, however, not as inert as a noble gas, as was initially assumed from atomic calculations.⁷

AUTHOR INFORMATION

Corresponding Author

*Tel.: +49-6131-39-25852. Fax: +49-6131-39-20811. E-mail: duellmann@uni-mainz.de.

Present Addresses

[†]A.Y.: Abteilung SHE Chemie, GSI Helmholtzzentrum für Schwerionenforschung, D-64291 Darmstadt, Germany.

[‡]J.M.G.: Nuclear Science Division, Lawrence Berkeley National Laboratory, Berkeley, CA 94720-8169, USA.

[▲]A.T.: Department of Chemistry & Biochemistry, University of Berne, CH-3012 Berne, Switzerland; and Laboratory for Radiochemistry and Environmental Chemistry, Paul Scherrer Institute, CH-5232 Villigen PSI, Switzerland.

[▼]M.S.: Advanced Science Research Center, Japan Atomic Energy Agency, Tokai, 319-1195 Ibaraki, Japan.

[★]J.D.: Sektion SHE Chemie, Helmholtz Institute Mainz, D-55099 Mainz, Germany.

[■]A.G.: Flerov Laboratory of Nuclear Reactions, Joint Institute for Nuclear Research, 141980 Dubna, Russian Federation.

[⊗]R.G.: Kerntechnische Anlagen, TÜV SÜD AG, 80686 München, Germany.

Author Contributions

The manuscript was written through contributions of all authors. All authors have given approval to the final version of the manuscript.

Notes

The authors declare no competing financial interest.

ACKNOWLEDGMENTS

We thank the ion source and accelerator staff for providing stable and intense beams, the GSI experimental electronic department for providing data acquisition and analysis software, and V. Pershina for valuable discussions. This work was

supported by the German BMBF under contracts 06MT247I, 06MT248, and 06MZ223I. The Research Center “Elementary Forces and Mathematical Foundations” is gratefully acknowledged.

REFERENCES

- (1) Fricke, B. *Struct. Bonding (Berlin, Ger.)* **1975**, *21*, 89.
- (2) Pyykkö, P.; Desclaux, J. P. *Acc. Chem. Res.* **1979**, *12*, 276.
- (3) Schwerdtfeger, P.; Seth, M. In *Encyclopedia of Computational Chemistry*; Schleyer, P. v. R., Allinger, N. L., Clark, T., Gasteiger, J., Schaefer, H. F., III, Schreiner, P. R., Eds.; Wiley: New York, 1998; Vol. 4.
- (4) Oganessian, Yu. *Radiochim. Acta* **2011**, *99*, 429–439.
- (5) Loss, R. D.; Corish, J. *Pure Appl. Chem.* **2012**, *84*, 1669–1672.
- (6) Türlér, A.; Pershina, V. *Chem. Rev.* **2013**, *113*, 1237.
- (7) Pitzer, K. S. *J. Chem. Phys.* **1975**, *63*, 1032.
- (8) Eichler, B. *Kernenergie* **1976**, *19*, 307.
- (9) Oganessian, Yu.; et al. *Phys. Rev. C* **2000**, *62*, 041604(R).
- (10) Eichler, B. *PSI Report 00-09*; Paul Scherrer Institute: Villigen, Switzerland, 2000.
- (11) Miedema, A. R.; Nieuwenhuys, B. E. *Surf. Sci.* **1981**, *104*, 491.
- (12) Eichler, R.; Schädel, M. *J. Phys. Chem. B* **2002**, *106*, 5413–5420.
- (13) Pershina, V. *Radiochim. Acta* **2011**, *99*, 459.
- (14) Pershina, V.; Anton, J.; Jacob, T. *J. Chem. Phys.* **2009**, *131*, 084713.
- (15) (a) Zaitsevskii, A.; van Wüllen, C.; Titov, A. *Russ. Chem. Rev.* **2009**, *78*, 1173. (b) Zaitsevskii, A.; et al. *Phys. Chem. Chem. Phys.* **2010**, *12*, 4152–4156.
- (16) Hermann, A.; et al. *Phys. Rev. B* **2010**, *82*, 155116.
- (17) Düllmann, Ch. E.; et al. *Nature* **2002**, *418*, 859–862.
- (18) Eichler, R.; et al. *Nature* **2007**, *447*, 72–75.
- (19) Eichler, R.; et al. *Angew. Chem. Int. Ed.* **2008**, *47*, 3262–3266.
- (20) Soverna, S.; et al. *Radiochim. Acta* **2005**, *93*, 1–8.
- (21) Yakushev, A.; et al. *Radiochim. Acta* **2003**, *91*, 433–437.
- (22) Oganessian, Y. *J. Phys. G* **2007**, *34*, R165–R242.
- (23) Düllmann, Ch. E.; et al. *Phys. Rev. Lett.* **2010**, *104*, 252701.
- (24) Stavsetra, L.; et al. *Phys. Rev. Lett.* **2009**, *103*, 132502.
- (25) Gates, J. M.; et al. *Phys. Rev. C* **2011**, *83*, 054618.
- (26) Ellison, P. A.; et al. *Phys. Rev. Lett.* **2010**, *105*, 182701.
- (27) Eichler, R.; et al. *Radiochim. Acta* **2010**, *98*, 133–139.
- (28) Eichler, B.; Zimmermann, H. P.; Gäggeler, H. W. *J. Phys. Chem. A* **2000**, *104*, 3126–3131.
- (29) Düllmann, Ch. E. *Radiochim. Acta* **2012**, *100*, 67–74.
- (30) Wittwer, D.; et al. *Nucl. Instrum. Methods Phys. Res., Sect. B* **2010**, *268*, 28–35.
- (31) Düllmann, Ch. E. *Eur. Phys. J. D* **2007**, *45*, 75–80.
- (32) Semchenkov, A.; et al. *Nucl. Instrum. Methods Phys. Res., Sect. B* **2008**, *266*, 4153–4161.
- (33) Dvorak, J.; et al. *Phys. Rev. Lett.* **2006**, *97*, 242501.
- (34) Eberhardt, K.; et al. *Nucl. Instrum. Methods Phys. Res., Sect. A* **2008**, *590*, 134–140.
- (35) Runke, J.; et al. *J. Radioanal. Nucl. Chem.* **2014**, *299*, 1081–1084.
- (36) Jäger, E.; et al. *J. Radioanal. Nucl. Chem.* **2014**, *299*, 1073–1079.
- (37) Ziegler, J. F. *Nucl. Instrum. Methods Phys. Res., Sect. B* **2004**, *219–220*, 1027.
- (38) Myers, W. D.; Świątecki, W. *J. Nucl. Phys. A* **1996**, *601*, 141.
- (39) Gregorich, K. E. *Nucl. Instrum. Methods Phys. Res., Sect. A* **2013**, *711*, 47–59.
- (40) Even, J.; et al. *Nucl. Instrum. Methods Phys. Res., Sect. A* **2011**, *638*, 157–164.
- (41) Zvara, I. *Radiochim. Acta* **1985**, *38*, 95–101.
- (42) Serov, A.; et al. *Proceedings of the Seventh International Conference on Nuclear and Radiochemistry*, Budapest, Hungary, 24–29 August, 2008; ISBN: 978-963-9319-81-3.
- (43) Brüchle, W. *Radiochim. Acta* **2003**, *91*, 71–80.